EJN European Journal of Neuroscience

FENS Federation of European Neuroscience Societies

European Journal of Neuroscience, Vol. 43, pp. 626–639, 2016 doi:10.1111/ejn.13157

MOLECULAR AND SYNAPTIC MECHANISMS

Peroxisome proliferator-activated receptor-γ coactivator-1α mediates neuroprotection against excitotoxic brain injury in transgenic mice: role of mitochondria and X-linked inhibitor of apoptosis protein

Johanna Mäkelä,[1,2,*] Giuseppa Mudò,[3,*] Dan Duc Pham,[1,2] Valentina Di Liberto,[3] Ove Eriksson,[1] Lauri Louhivuori,[4] Céline Bruelle,[1,2] Rabah Soliymani,[1] Marc Baumann,[1] Laura Korhonen,[1,5] Maciej Lalowski,[1] Natale Belluardo[3,†] and Dan Lindholm[1,2,†]

[1]Medicum, Department of Biochemistry and Developmental Biology, Medical Faculty, University of Helsinki, POB 63, 00014, Haartmaninkatu 8, FIN-00290 Helsinki, Finland

[2]Minerva Medical Research Institute, Biomedicum-2 Helsinki, Tukholmankatu 8, FIN-00290 Helsinki, Finland

[3]Department of Experimental Biomedicine and Clinical Neuroscience, Division of Human Physiology, University of Palermo, Corso Tukory 129, I-90134 Palermo, Italy

[4]Medicum, Department of Physiology, University of Helsinki, Helsinki, Finland

[5]Clinicum, Division of Child Psychiatry, Helsinki University Central Hospital, Helsinki, Finland

Keywords: kainic acid, mitochondria, neuron survival, PGC-1α, proteomics, XIAP

Edited by Deniz Kirik

Received 9 May 2015, revised 3 December 2015, accepted 29 December 2015

Abstract

Peroxisome proliferator-activated receptor gamma coactivator-1α (PGC-1α) is a transcriptional coactivator involved in the regulation of mitochondrial biogenesis and cell defense. The functions of PGC-1α in physiology of brain mitochondria are, however, not fully understood. To address this we have studied wild-type and transgenic mice with a two-fold overexpression of PGC-1α in brain neurons. Data showed that the relative number and basal respiration of brain mitochondria were increased in PGC-1α transgenic mice compared with wild-type mitochondria. These changes occurred concomitantly with altered levels of proteins involved in oxidative phosphorylation (OXPHOS) as studied by proteomic analyses and immunoblottings. Cultured hippocampal neurons from PGC-1α transgenic mice were more resistant to cell degeneration induced by the glutamate receptor agonist kainic acid. *In vivo* kainic acid induced excitotoxic cell death in the hippocampus at 48 h in wild-type mice but significantly less so in PGC-1α transgenic mice. However, at later time points cell degeneration was also evident in the transgenic mouse hippocampus, indicating that PGC-1α overexpression can induce a delay in cell death. Immunoblotting showed that X-linked inhibitor of apoptosis protein (XIAP) was increased in PGC-1α transgenic hippocampus with no significant changes in Bcl-2 or Bcl-X. Collectively, these results show that PGC-1α overexpression contributes to enhanced neuronal viability by stimulating mitochondria number and respiration and increasing levels of OXPHOS proteins and the anti-apoptotic protein XIAP.

Introduction

Mitochondria are important for producing cellular energy in the form of ATP via the process of oxidative phosphorylation. In addition, mitochondria are involved in regulation of cell metabolism, in the production of oxidative free radicals and in the control of intracellular calcium and of the intrinsic (mitochondria-dependent) pathway for cell death (Danial & Korsmeyer, 2004; Lindholm *et al.*, 2004; Cascone *et al.*, 2012; Nunnari & Suomalainen, 2012). Mitochondrial dysfunctions are observed during the course of several neurodegenerative diseases such as Parkinson′s disease (PD; Lin & Beal, 2006; Rugarli & Langer, 2012; Nunnari & Suomalainen, 2012). It has been proposed that boosting the number and functions of mitochondria can be beneficial in counteracting cell degeneration occurring in brain diseases (Houten & Auwerx, 2004; Handschin & Spiegelman, 2006).

Peroxisome proliferator-activated receptor-γ coactivator-1α (PGC-1α) is a master regulator of mitochondrial biogenesis and cell viabil-

Correspondence: Dan Lindholm, [1]Medicum, as above.
E-mail: dan.lindholm@helsinki.fi

*JM and GM contributed equally to this work.
†NB and DL contributed equally to this work.

ity (Austin & St-Pierre, 2012; Mudò *et al.*, 2012) and plays a role in the pathogenesis of PD and in Huntington's disease (Cui *et al.*, 2006; St-Pierre *et al.*, 2006; Weydt *et al.*, 2006; Zheng *et al.*, 2010). The precise mechanisms by which PGC-1α mediates neuroprotection are not fully understood. In addition to mitochondria, PGC-1α may influence cell signaling pathways, possibly in a cell- and tissue-specific manner.

In the present work, we have studied the role of mitochondria and PGC-1α in the control of neuronal viability using a model of excitotoxic brain injury caused by kainic acid (KA; Olney *et al.*, 1974; Korhonen *et al.*, 2001; Condorelli *et al.*, 2002). KA acts through KA–glutamate receptors on neurons causing neuronal damage particularly within specific regions in the hippocampus (Lerma, 2006). We studied hippocampus from wild-type and PGC-1α transgenic (tg) mice with overexpression of the transgene in neurons under the neuron-specific promoter *Thy1* (Caroni, 1997; Trapp *et al.*, 2003). We have previously shown that the midbrain dopaminergic neurons in the PGC1-tg mice are significantly protected against the deleterious effects of the neurotoxin 1-methyl-4-phenyl-1,2,3,6-tetrahydropyridine (MPTP) in the mouse model of PD (Mudò *et al.*, 2012). Using functional proteomics we analyzed the expression of mitochondrial proteins and how they might be changed by overexpression of PGC-1α in the brain neurons. The results showed that several proteins involved in oxidative phosphorylation (OXPHOS) were increased in the PGC-1α-tg mouse brain as compared to wild-type animals. In addition, the number and basal oxidative capacity of brain mitochondria were increased in the PGC-1α-tg mice.

Materials and methods

Animals

PGC-1α-tg mice expressing full-length PGC-1α with a Flag-tg in brain neurons were genotyped and bred in our animal house as described before (Mudò *et al.*, 2012). Experiments were approved by the ethical committees at the University of Helsinki and the University of Palermo and carried out in accordance with the European Communities Council Directive (86/609/EEC). Three-month-old male wild-type and PGC-1α-tg mice were injected with KA (Sigma, St Louis, MO, USA) into the lateral ventricle (0.35 μg/μL) in a volume of 0.5 μL as described (Sokka *et al.*, 2007; Putkonen *et al.*, 2011). Controls received equal volume of saline, and mice were killed at different times after injections. Wild-type and PGC-1α-tg mice were decapitated under deep anesthesia, and brains were rapidly dissected, frozen in isopentane, cooled in liquid nitrogen and stored at −70 °C until analysis. The right side of the brain was used for histology and the left for immunoblots.

TdT-mediated dUTP nick-end labeling (TUNEL) and Fluoro-Jade staining

TUNEL labeling and Fluoro-Jade staining were performed essentially as described previously (Korhonen *et al.*, 2001, 2005; Sokka *et al.*, 2007). In brief, for TUNEL labeling hippocampal sections from wild-type and PGC-1α-tg mice treated with KA or vehicle were fixed for 10 min with acetone : methanol (1:1) at −20 °C. The sections were then permeabilized with 0.1% Tween-20 and 1% bovine serum albumin in phosphate-buffered saline on ice. Fluorescein-labeled UTP (Roche, Basel, Switzerland) was added and sections incubated for 1 h at +37 °C, washed and analyzed under a fluorescence microscope (Zeiss, Germany). Hoechst staining (1 mg/mL, no. 33342; Sigma) was used to label cell nuclei. For Fluoro-Jade (0.001%; Histochem, Jackson, AR, USA) staining (Schmued *et al.*, 1997; Korhonen *et al.*, 2001; Chidlow *et al.*, 2009) the sections were immersed for 5 min in 1% sodium hydroxide in 80% ethanol, rinsed for 2 min in 70% ethanol, and then rinsed in distilled water. Potassium permanganate solution (0.06%) was added for 10 min, followed by a 10-min incubation in 0.0001% Fluoro-Jade C (Chemicon; Merck Millipore, Darmstadt, Germany). After staining, sections were washed in distilled water and mounted with Vectashield fluorescein-mounting medium (Vector Laboratories, Burlingame, CA, USA). The number of Fluoro-Jade- and TUNEL-positive cells was counted at the same bregma level in wild-type and treated mice (n = 4–8 for each time point).

Cresyl violet staining

For staining, mice were perfused with 4% paraformaldehyde in phosphate-buffered saline as described (Mudò *et al.*, 2012). Brains were dissected, dehydrated and embedded in paraffin using standard procedures. 10 μm brain sections from wild-type and PGC-1α-tg mice were dehydrated in an alcohol series, rehydrated in distilled water and stained in 0.3% Cresyl violet solution (Kebo, Sweden) for 15 s. Sections were rinsed in distilled water followed by an alcohol series, mounted with Entellan (Kebo) and analyzed using light microscopy (Korhonen *et al.*, 2005; Putkonen *et al.*, 2011).

Immunohistochemistry

For immunohistochemistry, 5-μm hippocampal sections from bregma −4.30 to −6.50 mm from control and PGC-1α-tg mice were obtained using a microtome (Microm HM240E; Thermo Scientific, Waltham, MA, USA) and collected on microscope slides. The slides were dried, deparaffinized and rehydrated in an alcohol series and water as above. For antigen retrieval, slides were heated in 10-mM citric acid solution at pH6 in a microwave oven for 5 min three times. Following three short washing steps, slides were incubated for 1 h with phosphate-buffered saline with 5% bovine serum albumin (Sigma) and 0.1% Triton-X-100 at room temperature. Primary PGC-1α (1:200; number ST1202; Merck Millipore, Billerica, MA, USA) and NeuN (1:300; MAB377; Merck Millipore) antibodies were then added overnight at +4 °C, followed by secondary Alexa 488- or 594-conjugated antibodies (1:500; Invitrogen, ThermoFisher, Waltham, MA, USA). Control samples were without primary antibodies. To label nuclei, Hoescht (Sigma) blue staining was used.

Quantitative PCR (qPCR)

Total RNA was extracted using the RNeasy lipid tissue kit (Qiagen, Hilden, Germany), followed by cDNA synthesis using Superscript VILO cDNA synthesis kit (Invitrogen) as described (Do *et al.*, 2012; Hyrskyluoto *et al.*, 2013). qPCR amplification was performed using a Light Cycler 480 II instrument (Roche Diagnostics, Basel, Switzerland) as described (Do *et al.*, 2012; Mäkelä *et al.*, 2014). Reactions were run in 96-well-plate format in a final volume of 10 μl and were optimized for maximal accuracy of quantification. The PCR reaction mixture contained 2 μL cDNA and 100 μM forward (F) and reverse (R) primers in 1× SYBR Green Master mix (Roche). The reaction was carried out at 95 °C for 10 min followed by at 95 °C for 15 s, 60 °C for 20 s and 72 °C for 10 s using 40 cycles. Each sample was run in triplicates on a 96-well plate and water was used as negative control. Expression levels were calculated based upon the $2^{-\Delta\Delta C}{}_{T}$ method using reference genes for β-actin and GAPDH that gave similar results. Primers used were:

PGC-1α: F, 5′-CAAACCAACAACTTTATC-3′ and R, 5′-TAGTCT TGTTCTCAAATG-3′; β-actin: F, 5′-CCTTCTTGGGTATGGAAT C-3′ and R, 5′-TGTTGGCATAGAGGTCTT -3′; GAPDH: F, 5′-CGACTTCAACAGCAACTC-3′ and R, 5′-TATTCATTGTCA TACCAG-GAA-3′.

Mitochondrial DNA copy number

DNA was isolated from wild-type and PGC-1α-tg mice using QIAamp DNA Mini Kit (Qiagen) according to the manufacturer's protocol. The relative mitochondrial DNA (mtDNA) copy number was measured using qPCR comparing the ratio of mtDNA to nuclear DNA as described before (Ylikallio *et al.*, 2010). In brief, the mitochondria-encoded *cytochrome-b (cytB* gene) was used for mtDNA and β-*actin* gene for nuclear DNA quantification. The primer sequences used were: for cytB, F, 5′-GCTTTCCACTTCATCT-TACCATTTA-3′ and R, 5′-TGTTGGGTTGTTTGATCCTG-3′; for β-actin: F, 5′-CCACCATGTACCCAGGCATT-3′ and R, 5′-ATCCCTGC-TTGCTGATCCAC-3′. The PCR reaction mixture contained 25 ng DNA and 100 nmol/L of F and R primers in 1× SYBR Green Master mix (Roche). The reaction was carried out at 95 °C for 10 min, then 40 cycles at 95 °C for 10 s and 60 °C for 30 s. Each sample was run in triplicate on a 96-well plate and water was used as negative control. qPCR amplification was performed using a Light Cycler 480 II instrument (Roche) as described (Mäkelä *et al.*, 2014). The ratio of mtDNA to nuclear DNA reflects the relative concentration of mtDNA.

Neuronal cultures

Hippocampal neurons were prepared from embryonic day (E)18 mouse from wild-type and PGC1-tg mice, and plated on poly-DL-ornithine (Sigma)-coated 96-well plates at a density of 40×10^3 cells. Cells were cultured in Neurobasal medium containing 2% B27 as described previously (Korhonen *et al.*, 2001; Sokka *et al.*, 2007; Kairisalo *et al.*, 2009; Putkonen *et al.*, 2011). Different concentrations of KA were added to the cultures for 24 h to induce cell degeneration (Korhonen *et al.*, 2001). Cell viability was determined by the MTT [3-(4,5-dimethylthiazol-2-yl)-2,5-diphenyltetrazolium bromide assay (Sigma) as described previously (Korhonen *et al.*, 2001; Sokka *et al.*, 2007; Reijonen *et al.*, 2010; Hyrskyluoto *et al.*, 2013). The assays were performed three times or more.

Calcium imaging

Hippocampal neurons plated on poly-DL-ornithine-coated 25-mm cover glasses were incubated with 4 μM fura-2 acetoxymethylester (Molecular Probes Invitrogen, Life Technologies Ltd, Paisley, UK) at 37 °C for 20 min in HEPES-buffered media (pH 7.4) consisting of (in mM): NaCl, 137; KCl, 5; KH_2PO_4, 0.44; $NaHCO_3$, 4.2; $CaCl_2$, 1; $MgCl_2$, 1; HEPES, 10; and glucose, 10 (all from Sigma-Adlrich). After incubation the cover glass was used as the bottom of an open 1-mL chamber as previously described (Louhivuori *et al.*, 2015). Using 340- and 380-nm light excitation filter changers under the control of the InCytIM-2 System (Intracellular Imaging Inc., Cincinnati, OH, USA) and a dichroic mirror (DM430; Nikon), light emission was measured through a 510-nm barrier filter with an integrating charge-coupled device camera (COHU Inc., Poway, CA, USA). A ratioed image of the ratio 340 : 380 nm was acquired each second. The data collected was analyzed with the InCyt 4.5 software (Intracellular Imaging Inc.) and further processed with Origin 6.0 software (OriginLabCorp, Northhampton, MA, USA).

Isolation of brain mitochondria and analyses of respiratory capacity

Mitochondria were isolated from brain tissue of wild-type and PGC-1α-tg mice as previously described (Speer *et al.*, 2003; Mudò *et al.*, 2012). Oxygen consumption measurements of isolated mitochondria were performed as described (Rogers *et al.*, 2011) with minor modifications. Mitochondria were suspended in a medium containing (in mM): sucrose, 250; Hepes-KOH pH 7.4, 10; EGTA, 1; Mg^{2+}, 3; Pi, 3; D-β-hydroxybutyrate, 5; and pyruvate, 5; the mitochondria were dispensed onto a Seahorse 96-well plate (Seahorse Bioscience, Boston, MA, USA) at a concentration of 40 μg protein per well. Mitochondria were sedimented by centrifugation at 2000 ***g*** for 20 min at +4 °C. The oxygen consumption rate (OCR) of mitochondria was determined in real-time using the Seahorse XF^e96 analyzer (Seahorse Bioscience) as previously described (Mäkelä *et al.*, 2014). ADP (1 mM) was added to the wells prior to the start of the experiment followed by the addition of 1 μM carbonyl cyanide 4-(trifluoromethoxy)phenylhydrazone (FCCP; mitochondrial uncoupler) and 1 μM rotenone (complex I inhibitor of the respiratory chain) plus 1 μM antimycin A (complex III inhibitor). Three measurements were done for each experimental condition, and experiments were repeated. The values obtained were normalized to the amount of mitochondrial protein determined in each sample.

Western blotting

Immunoblotting was done essentially as described previously (Korhonen *et al.*, 2001; Sokka *et al.*, 2007; Putkonen *et al.*, 2011; Hyrskyluoto *et al.*, 2014). In brief, hippocampal tissue from wild-type and PGC-1α tg mice was lysed using ice-cold RIPA buffer (NaCl, 150 mM; Triton-X-100, 1%; sodium deoxycholate, 0.5%; SDS, 1%; and Tris-HCl, pH 7.4, 50 mM) supplemented with protease inhibitor cocktail (Roche) and phosphatase inhibitors (PhoStop; Roche). Equal amounts of protein were subjected to SDS-PAGE and blotted onto nitrocellulose filters (Amersham Biosciences, Bucks, UK), which were incubated for 1 h in 5% skimmed milk or bovine serum albumin, in TBS-T (Tris-HCl, pH 7.5, 50 mM; NaCl, 150 mM; and Tween 20, 0.1%), and then with primary antibodies overnight at 4 °C. These included antibodies against Bcl-2 (diluted 1:1000; Cell Signaling Technology, Denvers, MA, USA; cat number 28769), Bcl-xL (1:1000; BD Transduction Laboratories, Franklin Lakes, NJ, USA; cat number B310211), GluR6/7 (1:1000; no. 04-921; Millipore/Upstate, Merck Millipore), PGC-1α (1:2000; Merck, Merck Millipore), X-linked inhibitor of apoptosis protein (XIAP; 1:5000; BD Biosciences, Franklin Lakes, NJ, USA) and β-actin (1:1000, number 2066; Sigma). After washing, the filter was incubated with horseradish peroxidase-conjugated secondary antibodies (1:2500; Jackson ImmunoResearch Laboratories, West Grove, PA, USA), followed by detection using enhanced chemiluminescence (Thermo, Waltham, MA, USA). Quantifications were done using the ImageJ software (version 1.410).

To study expression of respiratory change proteins we applied the OXPHOS antibody cocktail (diluted 1:250; no. 110413; Abcam, Cambridge, UK) for immunoblotting. This contains antibodies for proteins of the five respiratory chain complexes (I-V). Anti-porin antibody was used as a control. We further employed an antibody against ATP synthase-5β (kind gift from B. Battersby) to compare with data on ATP synthase-5α in complex V (Fig. 3).

Proteomic analyses

Sample preparation and proteolytic digestion

Ten micrograms of protein from control and PGC-1α-tg mice brains was digested using a modified FASP protocol (Scifo *et al.*, 2015). In brief, lysate buffer was exchanged by washing it several times with 8 M urea and 0.1 M Tris, pH 8 (urea buffer; UB). The proteins were reduced by addition of 10 mM DTT in UB, washed, alkylated with 50 mM iodoacetamide in UB, and 1:50 w/w of lysine-C endopeptidase (Wako, Richmond, VA, USA) was added in ~ 4 M urea with 0.1 M Tris, pH 8, followed by incubation overnight at room temperature. The peptide digest was collected by centrifugation, and trypsin solution was added in a ratio of 1:50 w/w in 50 mM ammonium bicarbonate. The peptide digests were cleaned using C18 reverse-phase ZipTip™ (Millipore), resuspended in 1% trifluoroacetic acid and sonicated for 1 min in a water bath.

Liquid chromatography (LC)–high definition mass spectrometry (HDMS)

Three-hundred nanograms of digested proteins (three technical replicates per sample) was used for LC-MS analysis. The peptides were separated with the nanoAcquity UPLC system (Waters) equipped with a 5-μm Symmetry C18 trapping column, 180 μm × 20 mm, reverse-phase (Waters), followed by an analytical 1.7-μm, 75 μm × 250 mm BEH-130 C18 reversed-phase column (Waters), in a single-pump trapping mode. The injected sample was trapped at a flow rate of 15 μL/min in 99.5% of solution A (0.1% formic acid), and the peptides were separated with a linear gradient of 3–35% of solution B (0.1% each of formic acid and acetonitrile), for 100 min at a flow rate 0.3 μL/min and a column temperature of 35 °C. The columns are flushed with an additional 5-min wash with up to 85% of solution B, followed by two empty runs to wash out any remaining peptides. The randomized samples were run in ion mobility-assisted data-independent analysis mode ($HDMS^E$), in a Synapt G2-S mass spectrometer (Waters), by alternating between low collision energy (6V) and a high collision energy ramp (20–45 V) in the transfer compartment and using a 1-s cycle time. The separated peptides were detected online with a mass spectrometer, operated in positive resolution mode in the range *m/z* 50–2000 amu. Human [Glu^1]-fibrinopeptide B (150 fmol/μL; Sigma) in 50% acetonitrile with 0.1% formic acid solution at a flow rate of 0.3 μL/min was used for a lock mass correction, applied every 30 s.

Database mining of LC-$HDMS^E$

Relative quantification between samples using precursor ion intensities was performed with TransOmics™ Informatics for Proteomics software (Nonlinear Dynamics, Waters) and ProteinLynx Global Server (PLGS V3.0). MS^E parameters were set as follows: low energy threshold of 135 counts, elevated energy threshold of 30 counts, and intensity threshold of precursor/fragment ion cluster 750 counts. To compare the control(s) to other subjects we utilized the between-subjects design scheme of TransOmics™ software. The ANOVA calculation applied by this scheme assumes that the conditions are independent and applies the statistical test that presumes the means of the conditions are equal. Database searches were carried out against the reviewed *Mus musculus* UniProtKB-SwissProt database (release 2014_04; 32538 entries) with the Ion Accounting algorithm and the following parameters: peptide and fragment tolerance, automatic; maximum protein mass, 500 kDa; min fragment ion matches per protein, ≥ 7; min fragment ion matches per peptide, ≥ 3; min peptide matches per protein, ≥ 1; primary digest reagent, trypsin; missed cleavages allowed, 2; fixed modification, carbamidomethylation C; variable modifications, phosphorylation of STY residues; oxidation of methionine (M) and false discovery rate (FDR), < 4%. Protein quantitation was performed entirely on non-conflicting protein identifications, using precursor ion intensity data and standardized expression profiles. For annotation of mitochondrial protein expression we implemented differential change in protein expression > 1.3-fold, ANOVA P value < 0.05 and two or more unique peptides for quantitation. The annotation of mitochondrial proteins was achieved with MitoMiner v3.1_2014-08**,** an integrated web resource of mitochondrial proteomics (http://mitominer.mrc-mbu.cam.ac.uk/). The MitoMiner database combines evidence for mitochondrial involvement derived from the MitoMiner Reference Set (all species, 12925 proteins), the MitoCarta Inventory (human and mouse, 2682 proteins), IMPI (Integrated Mitochondrial Protein Index) v.Q3_2014 (human, mouse, rat and cow, 6726 proteins), annotations from Gene Ontology cellular component, information from large-scale mass-spectrometry studies and mitochondrial targeting sequence predictions. In the final steps of the procedure we manually curated the datasets based on literature knowledge. The mitochondrial proteins were further analyzed using Ingenuity Pathways (www.ingenuity.com). Data on the mitochondrial protein changes are given in Table S1 and alterations in OXPHOS protein levels in Fig. 3.

Quantification and statistical analysis

Statistical comparisons were performed using one-way ANOVA followed by Bonferroni *post hoc* tests. Immunoreactive cells were counted in the hippocampus after KA injections using the public domain NIH image program (http://rbs.info.nih.gov/nih-image). Brains were analyzed and, for each animal, five non-overlapping areas within the dentate gyrus and the CA1 and CA3 regions of the hippocampus were counted. Values are expressed as mean ± SEM. For each time-point analyzed *in vivo*, 4–8 mice were used. Evaluation of the staining intensity per cell was done using the ImageJ Software.

Student's unpaired *t*-test was used for comparing immunoblots and neuronal cultures from wild-type and PGC-1α-tg mice. Experiments were repeated more than three times. $P \leq 0.05$ was considered significant. Values are expressed as mean ± SEM.

For proteomic analyses, differentially regulated pathways were calculated as described above and *P*-values corrected using the multiple-testing Benjamin–Hochberg procedure.

For annotation of mitochondrial protein expression, we implemented a differential change in protein expression of > 1.3-fold, ANOVA *P*-value < 0.05 and two or more unique peptides for quantitation.

Results

Characterization of tg PGC-1α-expressing mice

Using the neuron-specific *Thy1* promoter (Caroni, 1997; Trapp *et al.*, 2003) we generated mice with overexpression of PGC-1α in brain neurons (Mudò *et al.*, 2012). We have previously shown that the midbrain dopaminergic neurons in these mice are less vulnerable to treatment with neurotoxins such as MPTP (Mudò *et al.*, 2012). Transgenic expression using the *Thy1* promoter can vary between different neuronal populations (Caroni, 1997) so we characterized the expression of PGC-1α in brain cortex and hippocampus of PGC-1α-tg mice. Quantitative PCR showed that the PGC-1α mRNA levels were increased about two-fold in hippocampus and brain cortex in PGC-1α-tg mice compared with wild-type animals (Fig. 1A). Furthermore,

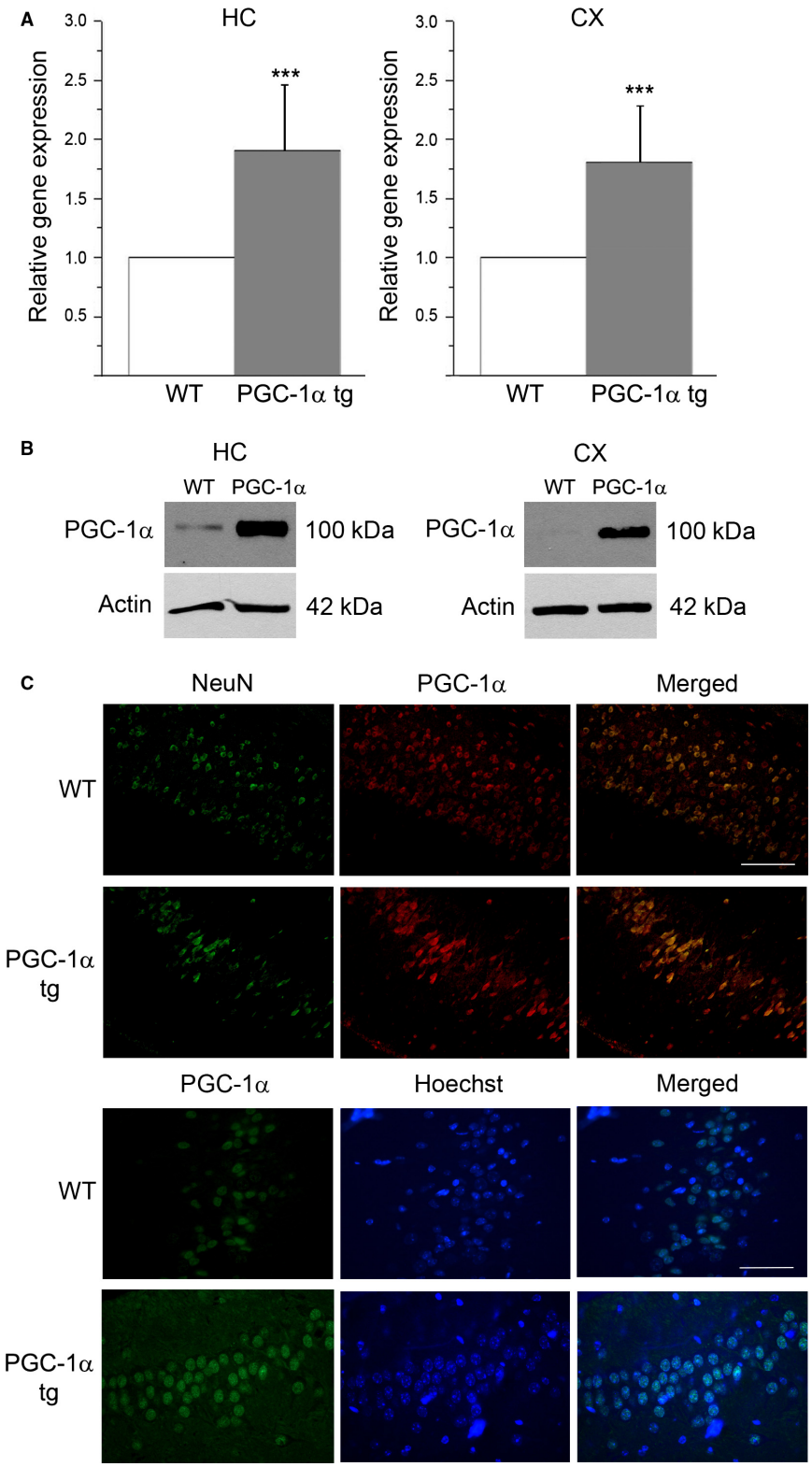

FIG. 1. PGC-1α is expressed in neurons in hippocampus and brain cortex of tg mice. (A) qPCR was performed using cDNA made from hippocampus (HC) and brain cortex (CX) of 3-month-old wild-type and PGC-1α-tg mice. Note a two-fold increase in PGC-1α expression in the tg mice compared with wild-type animals. Values are means ± SEM; $n = 4$, $^{***}P < 0.001$. (B) Immunoblotting using tissue lysates of HC and CX of wild-type and PGC-1α-tg mice. PGC-1α is shown as a band at 100 kDa and was increased in the PGC-1α-tg mice. A typical experiment is shown and this was repeated with similar results. (C) Sections were made from hippocampus of wild-type and PGC-1α-tg mice and immunostained using anti-PGC-1α antibodies. Upper panels, anti-PGC-1α (red fluorescence) antibodies were combined with anti-NeuN (green fluorescence) antibodies as a marker for neurons. Merged pictures (yellow) show co-staining of PGC-1α and NeuN in neurons in the CA3 region of hippocampus. Lower panels, anti-PGC-1α antibody (green fluorescence) was combined with Hoescht blue staining as a marker for nuclei. PGC-1α was present in most of the cell nuclei in the CA3 region. Scale bars, 100 μm (upper), 50 μm (lower).

the protein levels of PGC-1α were substantially increased in the PGC-1α-tg mice (Fig. 1B). To study the expression of PGC-1α at the cellular level, we performed double staining using anti-PGC-1α and anti-NeuN antibodies, the latter being a marker for neurons. Data showed that PGC-1α is expressed by neurons in the CA3 area of hippocampus in PGC-1α-tg and wild-type hippocampus (Fig. 1C). The calculated relative intensity of staining using the anti-PGC-1α antibody was significantly increased in hippocampal (1.25 ± 0.001, $^{***}P < 0.001$, $n = 4$) and in cortical (2.96 ± 0.008, $^{***}P < 0.001$, $n = 4$) neurons in PGC-1α-tg mice compared with wild-type animals. Immunolabeling of PGC1α combined with Hoescht blue staining revealed that PGC-1α is mainly nuclear; however, some immunoreactivity was also observed in the cytoplasm of neurons (Fig. 1C). This may reflect a possible regulatory step in PGC-1α physiology in neurons that requires mores studies in the future.

Mitochondrial number and oxidative respiration are increased in brains of PGC1-tg mice

PGC-1α plays a major role as an activator of mitochondrial biogenesis and cell viability (Houten & Auwerx, 2004; Handschin & Spiegelman, 2006; Austin & St-Pierre, 2012). We therefore studied the relative number of mitochondria in brains tissue of wild-type and PGC-1α-tg mice using qPCR (see Materials and Methods). Data showed that the content of mtDNA was increased in hippocampus in PGC-1α-tg mice compared with corresponding wild-type animals (Fig. 2A). We then studied the functions of mitochondria isolated from brain of wild-type and PGC-1α-tg mice using the Seahorse XF°96 analyzer. A graph from these experiments presented in Fig. 2B shows that the mitochondria from PGC-1α-tg mice had a higher basal OCR than did wild-type animals (Fig. 2B). The values obtained were normalized to the amount of mitochondrial protein and indicated that brain mitochondria in PGC-1α-tg mice are functionally more efficient than those in the wild-type animal using this assay. This result corroborates previous data showing an increased respiration of brain mitochondria in PGC-1α-tg mice (Mudò *et al.*, 2012).

Analyses of mitochondrial proteins in brains of PGC-1α-tg mice

To investigate protein changes in PGC-1α-tg mice in more detail, we performed functional proteomics analyses using mass spectrometry combined with bioinformatics, with a focus on mitochondrial proteins (see Materials and Methods). Canonical pathway analyses using Ingenuity Pathways and differentially expressed mitochondrial proteins (Table S1) pinpointed the mitochondrial dysfunctions and oxidative phosphorylation as being the statistically most associated pathways. Results showed that the relative abundance of several respiratory chain proteins involved in OXPHOS was altered in the PGC-1α-tg brain cortex as compared to wild-type cortex (Fig. 3A). The inset in Fig. 3A shows representative proteins of mitochondrial complex I (NDUFA10), complex II (SDHB), complex IV (COX5A) and complex V (ATP synthase-5I, -O and -8 proteins) that are increased in PGC-1α-tg brain cortex.

To validate our findings, we performed immunoblotting using isolated mitochondria from wild-type and PGC-1α-tg mice. The levels of SDHB in complex II and cytochrome c oxidase subunit I in complex IV were significantly increased in the PGC-1α-tg mouse mitochondria compared with wild-type mice (Fig. 3A and B). The changes in OXPHOS proteins in complex II were less evident using the antibodies available, whereas the level of NDUFB8 appeared to be decreased in the PGC-1α-tg mouse mitochondria (Fig. 3A and B). Proteomic analyses on whole brain cortex demonstrated dysregulation in expression of several subunits of the ATP synthase in the mitochondrial complex V, in the PGC-1α-tg brain (Table S1). With the antibodies against the ATP synthase subunits 5α and 5β (ATP5A1 and ATP5B; Fig. 3B) we observed a trend for upregulation of these components. Thus the mass spectrometric measurements revealed a similar increase in relative abundance, $P < 0.05$; not shown).

Taken together, these results show that neuronal overexpression of PGC-1α affects the expression of OXPHOS proteins in the brain, which affects the mitochondrial bioenergetics in these cells. Our proteomic analyses also revealed that proteins other than the OXPHOS ones were altered in the brains of PGC-1α-tg mice, something that is probably of functional significance for control of neuronal viability.

PGC-1α protects against KA-induced excitotoxicity in vitro *with no change in GluR6 receptors or intracellular calcium levels*

Neurons are sensitive to cell degeneration induced by excessive stimulation of glutamate receptors occurring in epilepsy and other

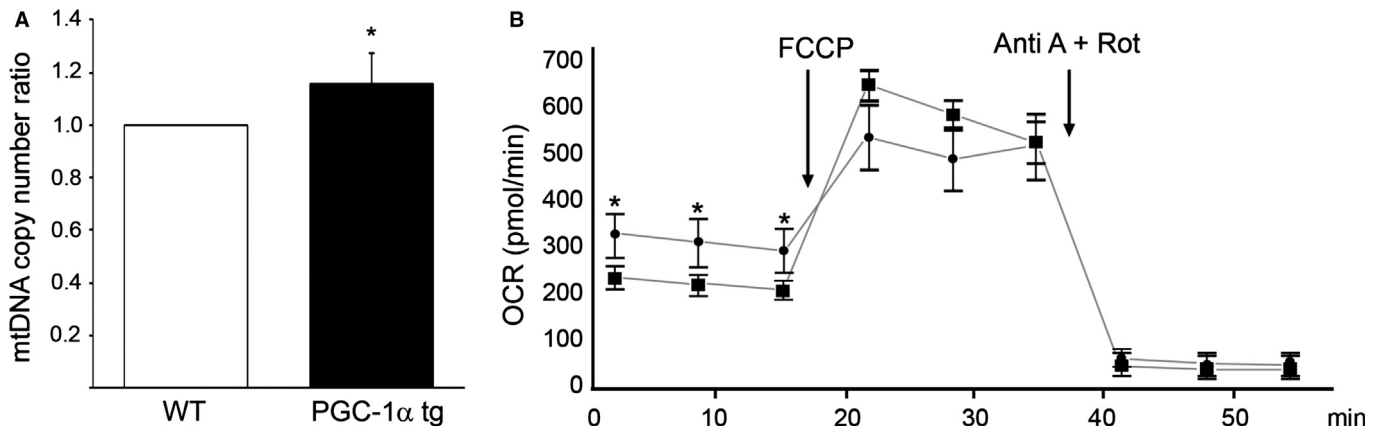

FIG. 2. Mitochondrial number and capacity are altered in PGC1-tg mouse brain. Three-month-old wild-type and PGC-1α-tg mice were used for analyzing the number and respiratory function of mitochondria as described. (A) DNA was isolated from brain tissue and mtDNA copy number was analyzed using qPCR. The relative mtDNA copy number was increased in brains of PGC-1α-tg compared with wild-type mice. Values are means ± SEM; $n = 3$, $^{*}P < 0.05$. (B) Mitochondria were prepared from brain cortex of wild-type and PGC-1α-tg mice. OCR by mitochondria was measured in real-time using the Seahorse XFe96 equipment. There was an increase in the basal OCR in PGC-1α-tg mitochondria compared with wild-type ones. Values are means ± SEM; $n = 6$, $^{*}P < 0.05$ for PGC-1α-tg mice vs. wild-type.

neurological disorders (Coyle & Putfarcken, 1993; Choi, 1994; Mattson, 2003). KA stimulates a specific class of glutamate receptors (GluRs) (Lerma, 2006), leading to neuronal cell death in hippocampus and some other areas of the brain (Olney *et al.*, 1974; Condorelli *et al.*, 2002). To study whether the overexpression of PGC-1α influences the cell responses towards KA we prepared hippocampal neurons from PGC-1α-tg and wild-type mice and cultured the cells for 7 days prior to KA treatment. Incubation of cells for 24 h with 10–100 μM KA increased cell death of hippocampal neurons from wild-type mice in a concentration-dependent manner (Fig. 4A) that is in line with previous data with rat hippocampal neurons (Korhonen *et al.*, 2001). In contrast, hippocampal neurons isolated from PGC-1α-tg mice were largely resistant to cell degeneration induced by KA (Fig. 4A). However, at a higher (300 μM) concentration of KA, hippocampal neurons from PGC-1α-tg mice also succumbed to cell death, indicating that the protection against excitotoxicity was not absolute.

To investigate whether the expression of the KA-responsive GluR, GluR6, is altered in the hippocampus we performed immunoblots using a specific antibody for this receptor (Putkonen *et al.*, 2011). Data showed that there was no difference in the levels of GluR6 in hippocampus between wild-type and PGC-1α-tg mice using an antibody recognizing both GluR6 and GluR7 subtypes of glutamate receptors (Fig. 4B). This suggests that the neuroprotection afforded by PGC-1α is not reflected by an altered level of GluR6/7. We then studied whether intracellular calcium levels are differentially increased by KA in neurons from wild-type and PGC-1α-tg mice. Fig. 4C and D shows that KA equally increased calcium levels in wild-type and PGC-1α-overexpressing neurons. It is still possible, however, that subtle differences may occur in calcium handling in these cells, particularly with regard to mitochondria or endoplasmic reticulum. This issue will require more details studied of wild-type and PGC-1α overexpressing neurons in the future.

PGC-1α induces a partial neuroprotection against excitotoxic neuronal damage in vivo

Next we studied changes in neuronal viability *in vivo* by injecting KA into the brains of wild-type and PGC-1α-tg mice. Hippocampal subregions, such as the C3 area, are particularly vulnerable to KA-induced neuronal excitotoxicity, as also shown here by an increase in the number of pycnotic cells revealed by Nissl staining (Fig. 5A). Similar results were obtained by using Fluoro-Jade to analyze neuronal degeneration (Korhonen *et al.*, 2005; Sokka *et al.*, 2007). Thus, KA induced a significant increase in Fluoro-Jade labeling in the CA3 region of wild-type mice at 48 h post-injection but less of an increase in PGC-1α-tg mice (Fig. 5B). However, at 72 h post-injection cells in the CA3 region of PGC-1α-tg mice also became labeled with Fluoro-Jade, a sign of ongoing cell degeneration. At this time point the relative number of Fluoro-Jade-positive cells in the CA3 and CA1 regions in PGC-1α-tg mice exceeded the corresponding numbers observed in wild-type mice (Fig. 5C).

To corroborate our findings with Fluoro-Jade, we employed TUNEL staining to detect DNA breaks as a marker of degenerating and dying neurons. Data showed that the number of TUNEL-positive cells induced by KA increased to a maximum at 48 h in the CA3 area of wild-type animals (Fig. 6A). In contrast, the number of TUNEL-positive cells was much less in the CA3 area in the PGC-1α-tg mice at this time point (Fig. 6A). At 72 h the number TUNEL-positive cells was about equal in the CA3 area in PGC-1α-tg and wild-type mice (Fig. 6A). In the CA1 region, the number of TUNEL-positive cells was less than in the CA3 region and the difference between PGC-1α-tg and wild-type mice was not as dramatic (Fig. 6B). In the dentate gyrus and hilus regions, few scattered cells became TUNEL-positive in both wild-type and PGC-1α-tg mice (Fig. 6C). These results on TUNEL labeling revealed a partial protection of hippocampal neurons against KA excitotoxicity in the PGC-1α-tg mice, particularly in the CA3 region. This is in agreement with data on Fluoro-Jade labeling above, and shows that neuronal degeneration induced KA was not totally abolished but rather delayed in the PGC-1α-tg mice.

Expression of anti-apoptotic proteins in hippocampus of control and PGC1-tg mice

In view of the protective effect observed with KA in the PGC-1α-tg mice we analyzed the levels of some well-known cell survival proteins in these animals. Western blotting revealed no significant changes in the levels of Bcl-2 and Bcl-xL in hippocampus of PGC-1α-tg compared with wild-type mice (Fig. 7A and B). In contrast, XIAP was significantly increased in hippocampus of PGC-1α-tg mice (Fig. 7C), suggesting that elevated XIAP may mediate part of the neuroprotection. This finding is in line with previous data on the roles of XIAP in KA-induced neurodegeneration (Korhonen *et al.*, 2001) and in brain ischemia (Trapp *et al.*, 2003).

Discussion

The present results show that overexpression of PGC-1α in brain neurons leads to a partial protection against KA-induced neuronal degeneration. This was shown by using Fluoro-Jade and by TUNEL labeling to identify degenerating neurons in the hippocampus of wild-type and PGC-1α-tg mice. TUNEL staining is a well-established method for detection of DNA breaks in dying cells and Fluoro-Jade is widely used to reveal nerve cell degeneration (Schmued

FIG. 3. Proteomic and immunoblot analyzes of mitochondria and OXPHOS proteins in wild-type and PGC-1α-tg mice. (A) Proteomics. Upper panel, differentially expressed mitochondria-associated proteins in brain cortex of wild-type and PGC-1α-tg mice were analyzed. Two canonical pathways are presented (rectangle) with the highest predicted *P*-values (*P*-values were corrected using the multiple-testing Benjamin–Hochberg procedure): the mitochondrial dysfunction and OXPHOS pathways. Selected OXPHOS proteins are shown with proportional change values given in the inset. Lower panel, OXPHOS proteins in complexes II, IV and V were upregulated in PGC-1α-tg brain cortex, as shown by the arrows. COX5A, cytochrome c oxidase subunit 5A; SDHB, succinate dehydrogenase (ubiquinone) iron-sulfur subunit; NDUFA10, NADH dehydrogenase [ubiquinone] 1 α subcomplex subunit 10; ATP5O, ATP synthase subunit O; ATP5I, ATP synthase subunit e, mitochondrial; ATP8, ATP synthase protein 8. (B) Immunoblots. Expression of mitochondrial OXPHOS proteins was analyzed by immunblotting using an antibody cocktail against specific proteins in the complex I-V (CI-V). Anti-porin antibody was used as a control. NDUFB8, NADH dehydrogenase (ubiquinone) 1β subunit 8 in CI; SDHB, succinate dehydrogenase in CII; UQCRC2, ubiquinol-cytochrome c reductase complex core protein in CIII; MTCO1, cytochrome c oxidase catalytic subunit 1 in CIV; ATP5A, ATP synthase subunit 5α in CV. Left panel, immunoblot with short exposure showing data on CII and CV. Immunoblot using an antibody against ATP synthase subunit 5β was also included. Right panels, immunoblot with longer exposure shows data on CIII, CIV and CI. (C) Quantification. Note increases in CII and CIV proteins in PGC-1α-tg mouse mitochondria compared with corresponding wild-type. No significant changes were observed for the CIII and CV proteins analyzed, whereas the NDUFB8 protein in CI was decreased as shown by the immunoblots. Values are means ± SEM; $n = 3$, $^{**}P < 0.01$.

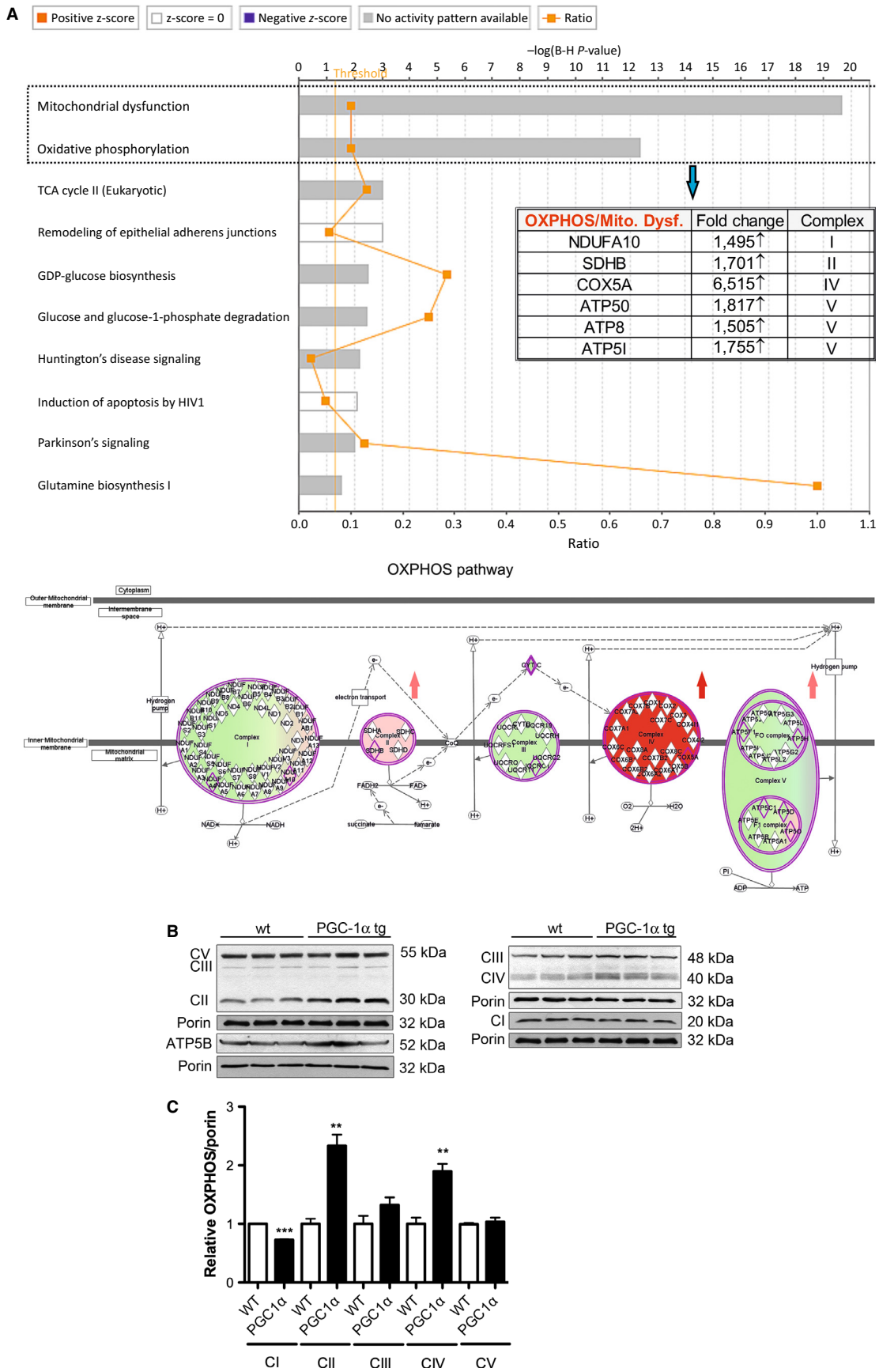

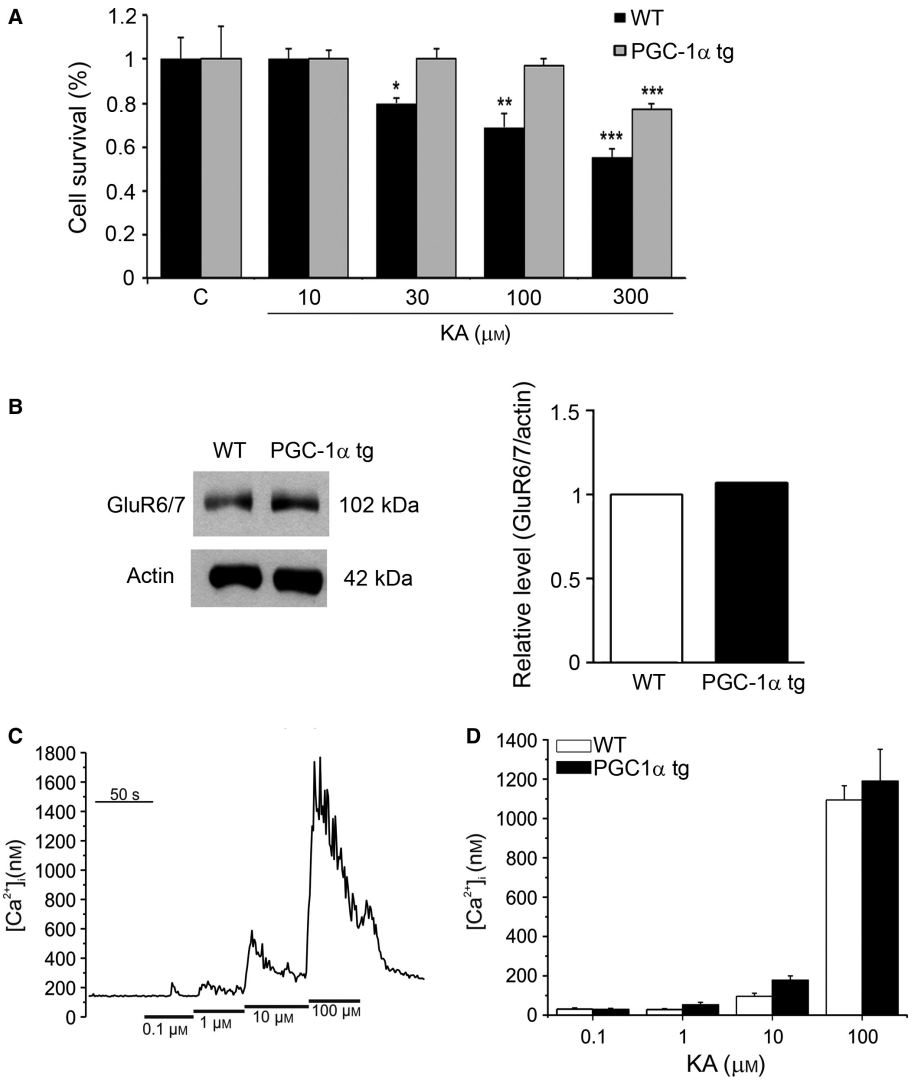

FIG. 4. PGC-1α overexpression does not influence either GluR6 or changes in intracellular calcium in hippocampal neurons but does protect against KA-induced cell damage. (A) Hippocampal neurons were prepared from embryonic day 18 wild-type and PGC-1α-tg mice. Cells were cultured for 7 days, followed by the addition of increasing amounts of KA for 24 h. Cell viability was analyzed using the MTT assay. KA induced cell degeneration in a concentration-dependent manner in wild-type neurons starting from 30 μM. PGC-1α-tg neurons were largely protected against KA, with a loss of cell viability at 300 μM KA. Values are means ± SEM; $n = 3$, $^{***}P < 0.001$, $^{**}P < 0.01$ and $^{*}P < 0.05$ for KA-treated vs. non-treated controls. (B) Immunoblots using hippocampal lysates from wild-type and PGC-1α-tg mice using specific antibodies against GluR6/7. There was no significant change in expression between these mice; $n = 4$. (C and D) Calcium imaging using Fura-2. (C) A representative calcium imaging trace of a typical response towards increasing concentrations of KA. (D) Statistics of the calcium response to different KA concentrations (0.1–100 μM). Quantification. Total number of neurons analyzed: wild-type, 146 and PGC-1α-tg, 141 in three different experiments. There was no significant change in intracellular calcium at any concentration of KA used for treatment. Values are means ± SEM; $n = 3$.

et al., 1997; Korhonen *et al.*, 2001; Chidlow *et al.*, 2009), although the precise substrate for this compound in neurons is not fully characterized. In this study these two methods overlapped with respect to changes in the number and spatial and temporal distribution of degenerating neurons in hippocampal subfields, with the largest KA-induced changes observed in the CA3 area of wild-type animals.

Mitochondria are the major source of energy in the cell and neuronal survival depends on proper function of these organelles (Lin & Beal, 2006; Rugarli & Langer, 2012). PGC-1α plays a crucial role in regulating biogenesis of mitochondria and cell protection against oxidative and other types of stress (Puigsever & Spiegelman, 2003; St-Pierre *et al.*, 2006). In the present work, we studied mechanisms for neuroprotection of PGC-1α-tg mice and attributed these to changes in mitochondria with an increased relative number of these organelles and with a higher basal capacity for oxygen consumption.

Previous studies have shown that neurons in PGC-1α gene-deleted mice are more vulnerable to oxidative stress and to neurotoxins such as KA and MPTP (St-Pierre *et al.*, 2006). Along with this we show here that increased PGC-1α expression in the PGC-1α-tg mice afforded a substantial neuroprotection against the deleterious effects of KA, as studied in hippocampal neurons *in vitro* and *in vivo*. This result substantiates previous data on the protective role of tg-expressed PGC-1α in dopaminergic neurons in the mouse model of PD (Mudò *et al.*, 2012). Together, these studies support the view that an increase in PGC-1α is beneficial for promoting survival of neurons under stressful conditions by the neurotoxins. How-

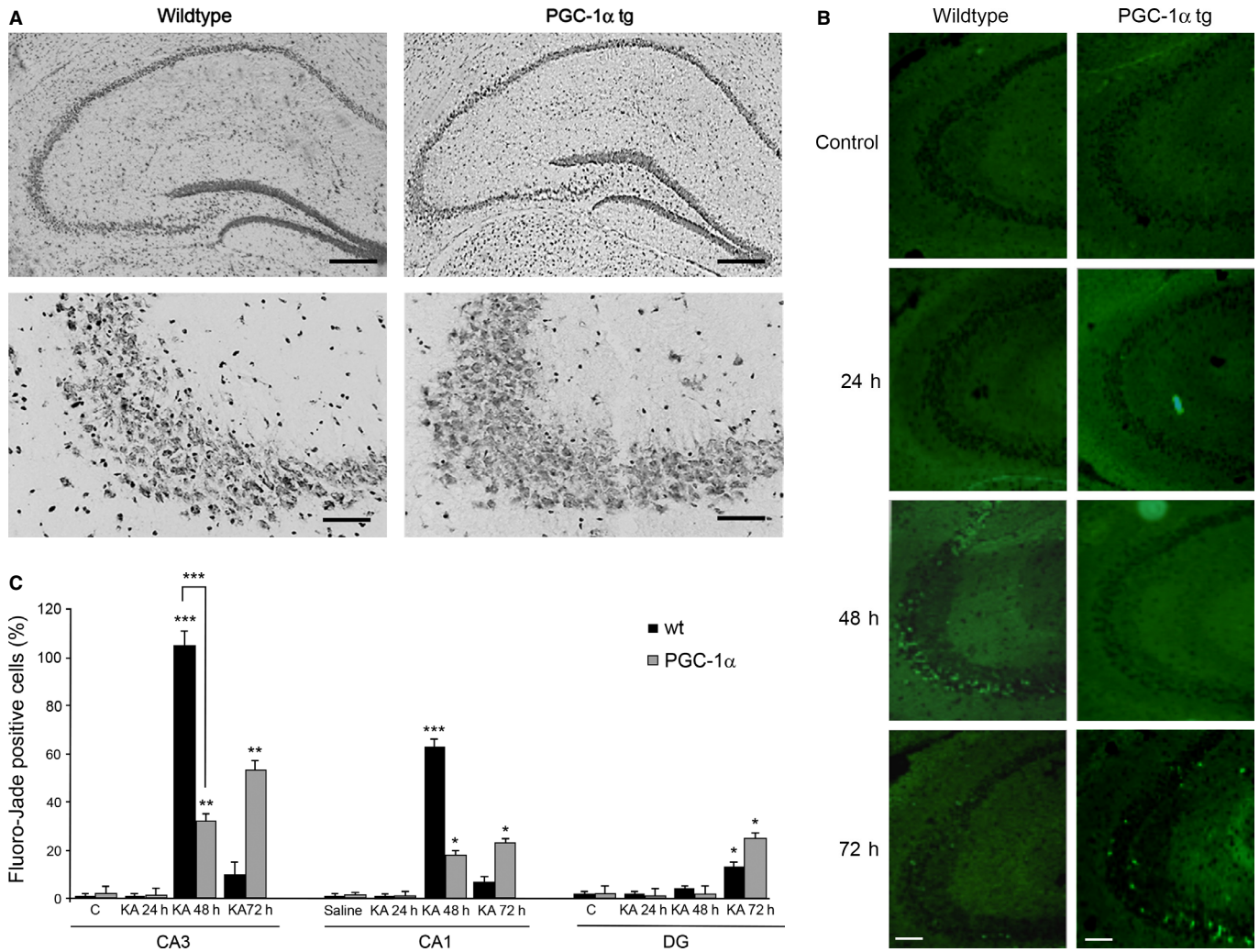

FIG. 5. PGC-1α affords neuroprotection against KA-induced exictotoxicity *in vivo*. Wild-type and PGC-1α-tg 3-month-old male mice were injected with KA for different time periods. Controls received an equal volume of saline. Hippocampal sections were made at each time point and analyzed further as indicated. (A) Nissl staining of hippocampal sections. Upper panels, whole hippocampus. Lower panels, higher magnification of the CA3 area. Note an increase in the number of pycnotic nuclei (shown as dark points) in wild-type mice following KA. (B) Fluoro-Jade staining (green fluorescence) shows cell degeneration in the moue hippocampus. Time course of Fluoro-Jade staining in the CA3 area of the hippocampus: Fluoro-Jade-positive cells are present in wild-type mice at 48 h but less so in PGC-1α-tg mice. The number of Fluoro-Jade-stained cells increased at 72 h in the PGC-1α-tg mice and decreased in the wild-type mice. (C) Quantification. The number of Fluoro-Jade-positive cells in the hippocampal subregions CA1, CA3 and DG were analyzed separately and counted. Values are means ± SEM; $n = 3$, $^{***}P < 0.001$, $^{**}P < 0.01$ and $^{*}P < 0.05$ for KA-treated vs. corresponding control saline; $^{**}P < 0.01$ for 48 h KA-treated CA3 and CA1 areas in wild-type mice vs. PGC-1α-tg mice. Scale bars, 1 mm (A, upper), 100 μm (A, lower), 75 μm (B).

ever, as also shown here the neuroprotection induced by PGC-1α against KA was not complete. Thus, cell degeneration of susceptible neurons also occurred in the hippocampus of PGC-1α-tg mice, albeit with a significant delay. The reason for this is not clear at the moment but could be due to the fact that the increases in mitochondrial number and viability were modest and not sufficient for long-term neuroprotection. KA is known to influence other pathways than mitochondria that may contribute to cell death in neurons. In this regard we have previously shown that KA induces changes in the endoplasmic reticulum (ER) with increased ER stress causing neuronal degeneration (Sokka *et al.*, 2007). Increased cell degeneration in the CA3 regions in PGC-1α-tg mice at later time points could also be due to the overactivation by KA of other neuronal cells in the brain, which in a circuit-dependent manner cause death of CA3 hippocampal neurons. It is further possible that the mode of cell death changes with time such that necrotic pathways become more prevalent at later time points and these are not rescued by mitochondria. In favor of such an interpretation we noted that the staining with Fluoro-Jade was still relatively high at 72 h post-treatment compared with the corresponding number of TUNEL-positive cells in the CA3 and CA1 regions of hippocampus (cf. Fig. 5A and B vs. Fig. 4C). Whatever the underlying mechanisms, it seems that a two-fold increase in PGC-1α mRNA is not enough to ensure complete neuroprotection, at least in the context of excitotoxic injury. This issue will require further studies with expression of higher levels of PGC-1α in the neurons. However, it should also be taken into account that a too high expression, as observed after viral delivery of PGC-1α into brain tissue, can itself cause neuronal degeneration (Ciron *et al.*, 2012; Clark *et al.*, 2012). These effects may be explained by an overstimulation of mitochondria related to high levels of PGC-1α and perhaps causing increased oxidative damage (for a discussion see Lindholm *et al.*, 2012). Hence it is pertinent to study the optimal physiological levels of PGC-1α in neurons, and how these can be attained by the use of drugs, substances and other

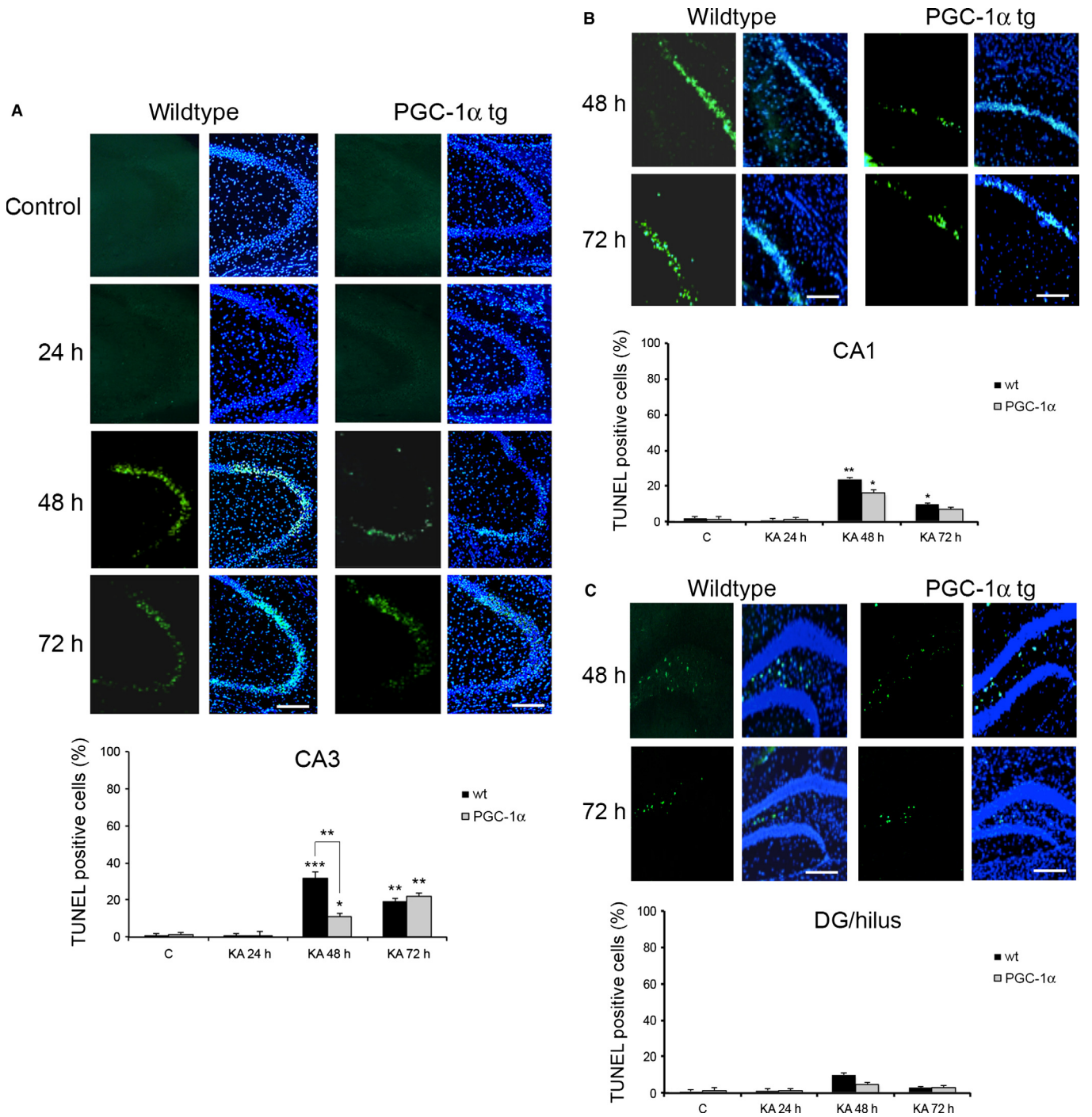

FIG. 6. TUNEL-labeled cells in the hippocampus of wild-type and PGC-1α-tg mice. Hippocampal sections were prepared from wild-type and PGC-1α-tg mice after treatment with KA or saline for different times. TUNEL staining was analyzed in different hippocampal areas. (A) Upper panels. Representative images of the time course of TUNEL labeling in the CA3 area of the hippocampus. Left, TUNEL-positive cells were present in wild-type mice at 48 h and less so in PGC-1α-tg mice. Right, Hoechst staining was done to label nuclei. Lower panel. Quantification shows the relative number of TUNEL-positive cells to Hoechst blue-positive nuclei. Values are means ± SEM; $n = 3$, $^{***}P < 0.001$, $^{**}P < 0.01$ and $^{*}P < 0.05$ for KA-treated vs. corresponding control saline; $^{**}P < 0.01$ for 48 h KA-treated CA3 wild-type vs. PGC-1α-tg mice. (B) Number of TUNEL-positive cells in the CA1 region. Upper panel, representative images at 48 and 72 h after KA. Lower panel, quantification as above. Values are means ± SEM; $n = 3$, $^{**}P < 0.01$ and $^{*}P < 0.05$ for KA-treated vs. control saline. (C) The number of TUNEL-positive cells in the dentate gyrus and hilus region. Upper panel, representative images at 48 h and 72 h after KA. Lower panel, quantification as above. Values are means ± SEM; $n = 3$, $^{*}P < 0.05$ for KA-treated vs. control saline. Scale bars, 50 μm.

factors in order to achieve a beneficial effect of PGC-1α in various brain diseases.

As a transcriptional cofactor PGC-1α plays a role in the expression of various genes. We were therefore interested to study which particular sets of proteins and particularly associated with mitochondria are changed in the PGC-1α-tg mice. Using mass spectrometry combined with bioinformatics tools we examined the mitochondria proteome of wild-type and PGC-1α-tg mice. Data showed that par-

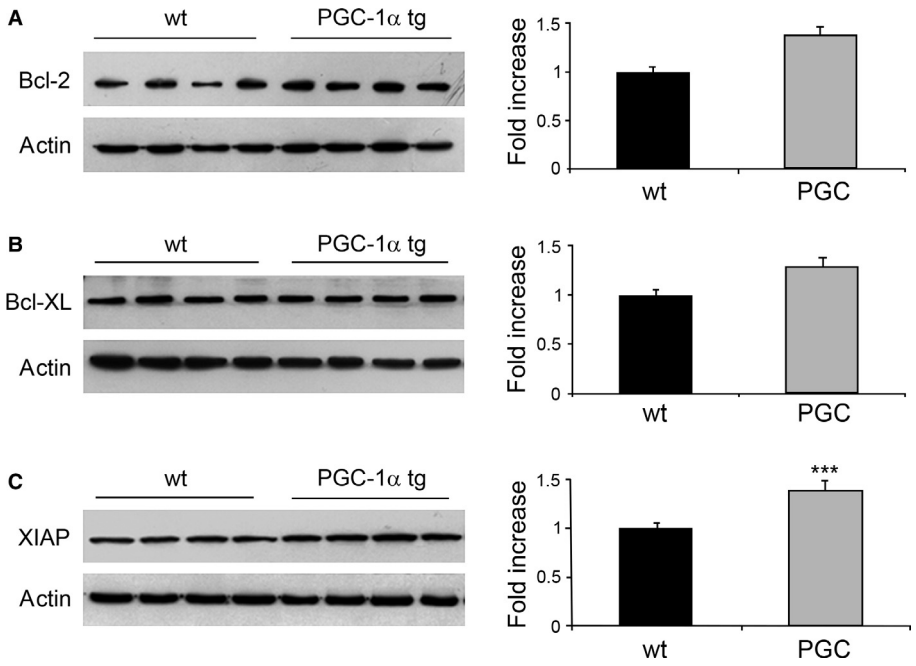

FIG. 7. Expression of anti-apoptotic proteins in the hippocampus of wild-type and PGC-1α-tg mice. Immunoblots using hippocampal lysates from wild-type and PGC-1α-tg mice using specific antibodies as indicated. β-actin was used as control. Lanes 1-4, wild-type animals; lanes 5-8, PGC-1α-tg mice. Values are means ± SEM; $n = 4$, $^{***}P < 0.001$. (A and B) There were no significant changes in the levels of (A) Bcl-2 or (B) BclxL between the groups. (C) XIAP was significantly increased in the PGC-1α-tg mice compared with wild-type animals.

ticularly OXPHOS proteins were altered in PGC-1α-tg compared with wild-type mice, but PGC-1α had a large effect on the mitochondrial proteome in neurons. Of the respiratory proteins analyzed particularly SDHB in complex II and the cytochrome c oxidase subunit I in complex IV were increased in PGC-1α-tg mice (Fig. 3). This reflects the enhanced basal respiration in PGC-1α mice overexpression in brain neurons. The present findings showing alterations in mitochondrial proteins in the PGC-1α-tg mice complement previous studies on the role of PGC-1α in regulation of OXPHOS proteins in brain tissue of PD patients (Zheng *et al.*, 2010). In addition to brain diseases, PGC-1α-regulated genes play an important role in metabolic diseases including type 2 diabetes (Mootha *et al.*, 2003).

In contrast to SDHB, we observed that NDUFB8 in complex I was downregulated in the PGC-1α-tg mice. This was also the case for NDUFA4 but not for NDUFA10 (Table S1). Complex I is a supramolecular complex composed of 45 protein subunits, and it is possible that the various subunits are differentially regulated by PGC-1α. Interestingly, it was recently shown that lower levels of free complex I components can increase substrate utilization and reduces production of oxygen free radicals during respiration (Miwa *et al.*, 2014). In view of this, the observed decreases in complex I proteins may influence free radical production and contribute to an increased resilience of neurons against toxin-induced cell death, but this warrants more studies in the future.

Seizures induced by KA are known to alter intracellular pathways related to induction of intracellular calcium and cell death (Korhonen *et al.*, 2001; Belluardo *et al.*, 2002; Mattson, 2003; Sokka *et al.*, 2007; Bozzi *et al.*, 2011; Putkonen *et al.*, 2011; Henshall & Engel, 2013). KA acts via specific KA receptors such as GluR6/7 (Lerma, 2006; Putkonen *et al.*, 2011). We therefore analyzed whether the expression of GluR6/7 was altered by PGC-1α overexpression as a possible explanation for the neuroprotective effect observed with PGC-1α. Data showed that there was no change in GluR6/7 levels in hippocampus between wild-type and PGC-1α-tg mice. In addition, imaging experiments revealed that KA induced a similar increase in the intracellular calcium level in wild-type and PGC-1α-tg neurons. These together indicate that the neuroprotection afforded by PGC-1α against KA is not related to changes in the GluR6/7 or in the calcium levels in the neurons.

In view of this we also studied the levels of anti-apoptotic proteins in the hippocampus of wild-type and PGC-1α-tg mice. Among the anti-apoptotic proteins, Bcl-2 and Bcl-xL belong to the Bcl-2 protein family and act at the level of the mitochondria to increase cell survival (Adams & Cory, 1998; Korhonen *et al.*, 2003), whereas XIAP acts downstream of mitochondria to inhibit caspases (Deveraux *et al.*, 1997; Danial & Korsmeyer, 2004; Lindholm & Arumäe, 2004). We observed that the relative level of XIAP was significantly increased in the PGC-1α-tg mice compared with controls, whilst Bcl-2 and Bcl-xL levels were not. We have previously shown that tg expression of XIAP in brain neurons contributes to neuroprotection after brain ischemia (Trapp *et al.*, 2003; Fukuda *et al.*, 2004; Wang *et al.*, 2004; Zhu *et al.*, 2007). The present data suggests that the increased levels of XIAP play a role in protecting neurons against KA-induced cell degeneration in the hippocampus in PGC-1α-tg mice. However, as discussed above, the neuroprotection in these animals was only partial, suggesting that the XIAP-mediated cell survival is not sufficient to fully block neuronal cell death induced by KA. Likewise, XIAP overexpression failed to completely protect against motoneuron degeneration observed in mutant SOD1 mice as a model of familial amyotrophic lateral sclerosis (Wootz *et al.*, 2006).

One intriguing question raised by this study is the mechanism by which PGC-1α overexpression leads to elevation of XIAP. Previous studies have shown that increases in XIAP are associated with NF-κB signaling and oxidative stress regulation as well as with the upregulation of brain-derived neurotrophic factor in neurons (Kairisalo *et al.*, 2007, 2009, 2011). The issue is further complicated by

the notion that both transcriptional and posttranscriptional events influence protein levels of XIAP, partially via enhanced protein translation (Holcik *et al.*, 2000). We are currently studying the links between PGC-1α and other signaling pathways in hippocampal neurons of PGC-1α-tg animals.

In this study we have overexpressed the full-length PGC-1α in brain neurons of tg mice. Recent studies have observed the expression of isoforms of PGC-1α in different tissues including brain (Soyal *et al.*, 2012). The presence of these variants were linked to the age of onset of Huntington's disease, but their precise functions remain to be determined. Moreover, brain-specific PGC-1α isoforms have so far been described only for human brain tissue. It remains therefore to be studied whether these PGC-1α variants are also expressed in the mouse brain and what their physiological function may be in neurons compared with the canonical PGC-1α protein studied here.

In sum, we show here that tg expression of PGC-1α in brain neurons induces a partial neuroprotection in mouse hippocampus against excitotoxic injury caused by KA. Increases in the relative number and respiratory functions of brain mitochondria contribute to the enhanced neuronal viability. PGC-1α overexpression also elevated the anti-apoptotic protein XIAP and increased the levels of particular OXPHOS proteins in brain mitochondria. Our study of the time dependency also revealed that the neuroprotection was not complete as PGC-1α overexpression induced a delay in nerve cell death in the hippocampus. This is important and suggests that the modulation of PGC-1α expression and mitochondria pathways in brain diseases are time-dependent and should be combined with treatment strategies directed towards parallel and other targets for intervention. In this respect the PGC-1α-tg animals can offer a suitable model for further studies of signaling pathways and protective mechanisms in brain diseases.

Supporting Information

Additional supporting information can be found in the online version of this article:

Table S1. List of differentially expressed, mitochondria-associated proteins in the brain cortex of wildtype and PGC-1 α transgenic mice.

Conflict of interest

The authors declare no conflicts of interests.

Acknowledgements

We thank E. Jääskeläinen and K. Söderholm for excellent technical assistance, J Döhla for experiments with characterization of PGC-1α-tg mice, and M. Ljungberg for help with work on hippocampal neurons. We are grateful to B. Battersby for the anti-ATP5beta antibody. Supported by Academy of Finland, Sigrid Juselius, Liv och Hälsa, Finska Läkaresällskapet, Svenska Kulturfonden, Magnus Ehrnrooth Foundation, Parkinson Foundation Finland, and by Minerva Foundation and Progetti di Ateneo, University of Palermo. Confocal imaging was done at the Biomedicum Imaging Unit at the Biomedicum Helsinki.

Abbreviations

F, forward; KA, kainic acid; MPTP, 1-methyl-4-phenyl-1,2,3,6-tetrahydropyridine; mtDNA, mitochondrial DNA; OCR, oxygen consumption rate; OXPHOS, oxidative phosphorylation; PD, Parkinson′s disease; PGC-1α, peroxisome proliferator-activated receptor-γ coactivator-1α; qPCR, quantitative PCR; R, reverse; Tg, transgenic; TUNEL, TdT-mediated dUTP nick-end labeling; XIAP, X-linked inhibitor of apoptosis protein.

References

Adams, J.M. & Cory, S. (1998) The Bcl-2 protein family: arbiters of cell survival. *Science*, **281**, 1322–1326.

Austin, S. & St-Pierre, J. (2012) PGC1alpha and mitochondrial metabolism–emerging concepts and relevance in ageing and neurodegenerative disorders. *J. Cell Sci.*, **125**, 4963–4971.

Belluardo, N., Korhonen, L., Mudo, G. & Lindholm, D. (2002) Neuronal expression and regulation of rat inhibitor apoptosis protein-2 by kainic acid in the rat brain. *Eur. J. Neurosci.*, **15**, 87–100.

Bozzi, Y., Dunleavy, M. & Henshall, D.C. (2011) Cell signaling underlying epileptic behavior. *Front. Behav. Neurosci.*, **5**, 45.

Caroni, P. (1997) Overexpression of growth-associated proteins in the neurons of adult transgenic mice. *J. Neurosci. Meth.*, **71**, 3–9.

Cascone, A., Bruelle, C., Lindholm, D., Bernardi, P. & Eriksson, O. (2012) Destabilization of the outer and inner mitochondrial membranes by core and linker histones. *PLoS ONE*, **7**, e35357.

Chidlow, G., Wood, J.P., Sarvestani, G., Manavis, J. & Casson, R.J. (2009) Evaluation of Fluoro-Jade C as a marker of degenerating neurons in the rat retina and optic nerve. *Exp. Eye Res.*, **88**, 426–437.

Choi, D.W. (1994) Glutamate receptors and the induction of excitotoxic neuronal death. *Prog. Brain Res.*, **100**, 47–51.

Ciron, C., Lengacher, S., Dusonchet, J., Aebischer, P. & Schneider, B.L. (2012) Sustained expression of PGC-1α in the rat nigrostriatal system selectively impairs dopaminergic function. *Hum. Mol. Genet.*, **21**, 1861–1876.

Clark, J., Silvaggi, J.M., Kiselak, T., Zheng, K., Clore, E.L., Dai, Y., Bass, C.E. & Simon, D.K. (2012) Pgc-1α overexpression downregulates Pitx3 and increases susceptibility to MPTP toxicity associated with decreased Bdnf. *PLoS ONE*, **7**, e4892.

Condorelli, D.F., Mudo, G., Trovato-Salinaro, A., Mirone, M.B., Amato, G. & Belluardo, N. (2002) Connexin-30 mRNA is up-regulated in astrocytes and expressed in apoptotic neuronal cells of rat brain following kainate-induced seizures. *Mol. Cell Neurosci.*, **21**, 94–113.

Coyle, J.T. & Putfarcken, P. (1993) Oxidative stress, glutamate, and neurodegenerative disorders. *Science*, **262**, 689–695.

Cui, L., Jeong, H., Borovecki, F., Parkhurst, C.N., Tanese, N. & Krainc, D. (2006) Transcriptional repression of PGC-1alpha by mutant huntingtin leads to mitochondrial dysfunction and neurodegeneration. *Cell*, **127**, 59–69.

Danial, N.N. & Korsmeyer, S.J. (2004) Cell death: critical control points. *Cell*, **116**, 205–219.

Deveraux, Q.L., Takahashi, R., Salvesen, G.S. & Reed, J.C. (1997) X-linked IAP is a direct inhibitor of cell-death proteases. *Nature*, **388**, 300–304.

Do, H.T., Tselykh, T.V., Mäkelä, J., Ho, T.H., Olkkonen, V.M., Bornhauser, B.C., Korhonen, L., Zelcer, N. & Lindholm, D. (2012) Fibroblast growth factor-21 (FGF21) regulates low-density lipoprotein receptor (LDLR) levels in cells via the E3-ubiquitin ligase Mylip/Idol and the Canopy2 (Cnpy2)/Mylip-interacting saposin-like protein (Msap). *J. Biol. Chem.*, **287**, 12602–12611.

Fukuda, H., Fukuda, A., Zhu, C., Korhonen, L., Swanpalmer, J., Hertzman, S., Leist, M., Lindholm, D., Lannering, B., Björk-Eriksson, T., Marky, I. & Blomgren, K. (2004) Irradiation-induced progenitor cell death in the developing brain is resistant to erythropoietin treatment and caspase inhibition. *Cell Death Differ.*, **11**, 1166–1178.

Handschin, C. & Spiegelman, B.M. (2006) Peroxisome proliferator-activated receptor gamma coactivator 1 coactivators, energy homeostasis, and metabolism. *Endocr. Rev.*, **27**, 728–735.

Henshall, D.C. & Engel, T. (2013) Contribution of apoptosis-associated signaling pathways to epileptogenesis: lessons from Bcl-2 family knockouts. *Front. Cell Neurosci.*, **7**, 110.

Holcik, M., Yeh, C., Korneluk, R.G. & Chow, T. (2000) Translational upregulation of X-linked inhibitor of apoptosis (XIAP) increases resistance to radiation induced cell death. *Oncogene*, **19**, 4174–4177.

Houten, S.M. & Auwerx, J. (2004) PGC-1alpha: turbocharging mitochondria. *Cell*, **119**, 5–7.

Hyrskyluoto, A., Pulli, I., Törnqvist, K., Ho, T.H., Korhonen, L. & Lindholm, D. (2013) Sigma-1 receptor agonist PRE084 is protective against mutant huntingtin-induced cell degeneration: involvement of calpastatin and the NF-κB pathway. *Cell Death Dis.*, **4**, e646.

Hyrskyluoto, A., Bruelle, C., Lundh, S.H., Do, H.T., Kivinen, J., Rappou, E., Reijonen, S., Waltimo, T., Petersén, Å., Lindholm, D. & Korhonen, L. (2014) Ubiquitin-specific protease-14 reduces cellular aggregates and protects against mutant huntingtin-induced cell degeneration: involvement of

the proteasome and ER stress-activated kinase IRE1α. *Hum. Mol. Genet.*, **23**, 5928–5939.
Kairisalo, M., Korhonen, L., Blomgren, K. & Lindholm, D. (2007) X-linked Inhibitor of Apoptosis Protein increases mitochondrial antioxidants through NF-κB activation. *Biochem. Bioph. Res. Co.*, **364**, 138–144.
Kairisalo, M., Korhonen, L., Sepp, M., Pruunsild, P., Kukkonen, J.P., Kivinen, J., Timmusk, T., Blomgren, K. & Lindholm, D. (2009) NF-kappaB-dependent regulation of brain-derived neurotrophic factor in hippocampal neurons by X-linked inhibitor of apoptosis protein. *Eur. J. Neurosci.*, **30**, 958–966.
Kairisalo, M., Bonomo, A., Hyrskyluoto, A., Mudò, G., Belluardo, N., Korhonen, L. & Lindholm, D. (2011) Resveratrol reduces oxidative stress and cell death and increases mitochondrial antioxidants and XIAP in PC6.3-cells. *Neurosci. Lett.*, **488**, 263–266.
Korhonen, L., Belluardo, N. & Lindholm, D. (2001) Regulation of X-chromosome-linked inhibitor of apoptosis protein in kainic acid-induced neuronal death in the rat hippocampus. *Mol. Cell Neurosci.*, **17**, 364–372.
Korhonen, L., Belluardo, N., Mudo, G. & Lindholm, D. (2003) Increase in Bcl-2 phosphorylation and reduced levels of BH3-only proteins in kainic acid mediated neuronal death in the rat brain. *Eur. J. Neurosci.*, **18**, 1121–1134.
Korhonen, L., Hansson, I., Kukkonen, J.P., Brannvall, K., Kobayashi, M., Takamatsu, K. & Lindholm, D. (2005) Hippocalcin protects against caspase-12-induced and age-dependent neuronal degeneration. *Mol. Cell Neurosci.*, **28**, 85–95.
Lerma, J. (2006) Kainate receptor physiology. *Curr. Opin. Pharmacol.*, **6**, 89–97.
Lin, M.T. & Beal, M.F. (2006) Mitochondrial dysfunction and oxidative stress in neurodegenerative diseases. *Nature*, **443**, 787–795.
Lindholm, D. & Arumäe, U. (2004) Cell Differentiation: Reciprocal Regulation of Apaf-1 and the Inhibitor of Apoptosis proteins. *J. Cell Biol.*, **167**, 193–195.
Lindholm, D., Eriksson, O. & Korhonen, L. (2004) Mitochondrial proteins in neuronal degeneration. *Biochem. Bioph. Res. Co.*, **321**, 753–758.
Lindholm, D., Eriksson-Rosenberg, O., Mäkela, J., Belluardo, N. & Korhonen, L. (2012) PGC-1 alpha: a master gene that is hard to master. *Cell. Mol. Life Sci.*, **69**, 2465–2468.
Louhivuori, L.M., Jansson, L., Turunen, P.M., Jäntti, M.H., Nordström, T., Louhivuori, V. & Åkerman, K.E. (2015) Transient receptor potential channels and their role in modulating radial glial-neuronal interaction: a signaling pathway involving mGluR5. *Stem Cells Dev.*, **24**, 701–713.
Mäkelä, J., Tselykh, T.V., Maiorana, F., Eriksson, O., Do, H.T., Mudò, G., Korhonen, L.T., Belluardo, N. & Lindholm, D. (2014) Fibroblast growth factor-21 enhances mitochondrial functions and increases the activity of PGC-1α in human dopaminergic neurons via Sirtuin-1. *Springer Plus*, **3**, 2.
Mattson, M.P. (2003) Excitotoxic and excitoprotective mechanisms: Abundant targets for the prevention and treatment of neurodegenerative disorders. *NeuroMol. Med.*, **3**, 65–94.
Miwa, S., Jow, H., Baty, K., Johnson, A., Czapiewski, R., Saretzki, G., Treumann, A. & von Zglinicki, T. (2014) Low abundance of the matrix arm of complex I in mitochondria predicts longevity in mice. *Nat. Commun.*, **5**, 3837.
Mootha, V.K., Lindgren, C.M., Eriksson, K.F., Subramanian, A., Sihag, S., Lehar, J., Puigserver, P., Carlsson, E., Ridderstråle, M., Laurila, E., Houstis, N., Daly, M.J., Patterson, N., Mesirov, J.P., Golub, T.R., Tamayo, P., Spiegelman, B., Lander, E.S., Hirschhorn, J.N., Altshuler, D. & Groop, L.C. (2003) PGC-1alpha-responsive genes involved in oxidative phosphorylation are coordinately downregulated in human diabetes. *Nat. Genet.*, **34**, 267–273.
Mudò, G., Mäkelä, J., Liberto, V.D., Tselykh, T.V., Olivieri, M., Piepponen, P., Eriksson, O., Mälkiä, A., Bonomo, A., Kairisalo, M., Aguirre, J.A., Korhonen, L., Belluardo, N. & Lindholm, D. (2012) Transgenic expression and activation of PGC-1α protect dopaminergic neurons in the MPTP mouse model of Parkinson's disease. *Cell. Mol. Life Sci.*, **69**, 1153–1165.
Nunnari, J. & Suomalainen, A. (2012) Mitochondria: in sickness and in health. *Cell*, **148**, 1145–1159.
Olney, J.W., Rhee, V. & Ho, O.L. (1974) Kainic acid: a powerful neurotoxic analog of glutamate. *Brain Res.*, **77**, 507–512.
Puigsever, P. & Spiegelman, B.M. (2003) Peroxisome proliferator-activated receptor-gamma coactivator 1 alpha (PGC-1 alpha): transcriptional coactivator and metabolic regulator. *Endocr. Rev.*, **24**, 78–90.
Putkonen, N., Kukkonen, J., Mudo, G., Putula, J., Belluardo, N., Lindholm, D. & Korhonen, L. (2011) Involvement of cyclin-dependent kinase-5 in kainic acid-mediated degeneration of glutamatergic synapses in the rat hippocampus. *Eur. J. Neurosci.*, **34**, 1212–1221.
Reijonen, S., Kukkonen, J.P., Hyrskyluoto, A., Kivinen, J., Kairisalo, M., Takei, N., Lindholm, D. & Korhonen, L. (2010) Downregulation of NF-kappaB signaling by mutant huntingtin proteins induces oxidative stress and cell death. *Cell. Mol. Life Sci.*, **67**, 1929–1941.
Rogers, G.W., Brand, M.D., Petrosyan, S., Ashok, D., Elorza, A.A., Ferrick, D.A. & Murphy, A.N. (2011) High throughput microplate respiratory measurements using minimal quantities of isolated mitochondria. *PLoS ONE*, **6**, e21746.
Rugarli, E.I. & Langer, T. (2012) Mitochondrial quality control: a matter of life and death for neurons. *EMBO J.*, **31**, 1336–1349.
Schmued, L.C., Albertson, C. & Slikker, W. Jr (1997) Fluoro-Jade: a novel fluorochrome for the sensitive and reliable histochemical localization of neuronal degeneration. *Brain Res.*, **751**, 37–46.
Scifo, E., Szwajda, A., Soliymani, R., Pezzini, F., Bianchi, M., Dapkunas, A., Dębski, J., Uusi-Rauva, K., Dadlez, M., Gingras, A.-C., Tyynelä, J., Simonati, A., Jalanko, A., Baumann, M.H. & Lalowski, M. (2015) Proteomic analysis of the palmitoyl protein thioesterase 1 interactome in SH-SY5Y human neuroblastoma cells. *J. Proteomics.*, **123**, 42–53.
Sokka, A.L., Putkonen, N., Mudo, G., Pryazhnikov, E., Reijonen, S., Khiroug, L., Belluardo, N., Lindholm, D. & Korhonen, L. (2007) Endoplasmic reticulum stress inhibition protects against excitotoxic neuronal injury in the rat brain. *J. Neurosci.*, **27**, 901–908.
Soyal, S.M., Felder, T.K., Auer, S., Hahne, P., Oberkofler, H., Witting, A., Paulmichl, M., Landwehrmeyer, G.B., Weydt, P. & Patsch, W. (2012) European Huntington Disease Network. A greatly extended PPARGC1A genomic locus encodes several new brain-specific isoforms and influences Huntington disease age of onset. *Hum. Mol. Genet.*, **21**, 3461–3473.
Speer, O., Morkunaite-Haimi, S., Liobikas, J., Franck, M., Hensbo, L., Linder, M.D., Kinnunen, P.K., Wallimann, T. & Eriksson, O. (2003) Rapid suppression of mitochondrial permeability transition by methylglyoxal. Role of reversible arginine modification. *J. Biol. Chem.*, **278**, 34757–34763.
St-Pierre, J., Drori, S., Uldry, M., Silvaggi, J.M., Rhee, J., Jager, S., Handschin, C., Zheng, K., Lin, J., Yang, W., Simon, D.K., Bachoo, R. & Spiegelman, B.M. (2006) Suppression of reactive oxygen species and neurodegeneration by the PGC-1 transcriptional coactivators. *Cell*, **127**, 397–408.
Trapp, T., Korhonen, L., Besselmann, M., Martinez, R., Mercer, E.A. & Lindholm, D. (2003) Transgenic mice overexpressing XIAP in neurons show better outcome after transient cerebral ischemia. *Mol. Cell Neurosci.*, **23**, 302–313.
Wang, X., Zhu, C., Wang, X., Hagberg, H., Korhonen, L., Sandberg, M., Lindholm, D. & Blomgren, K. (2004) X-linked inhibitor of apoptosis protein (XIAP) protects against caspase activation and tissue loss after neonatal hypoxia-ischemia. *Neurobiol. Dis.*, **16**, 179–189.
Weydt, P., Pineda, V.V., Torrence, A.E., Libby, R.T., Satterfield, T.F., Lazarowski, E.R., Gilbert, M.L., Morton, G.J., Bammler, T.K., Strand, A.D., Cui, L., Beyer, R.P., Easley, C.N., Smith, A.C., Krainc, D., Luquet, S., Sweet, I.R., Schwartz, M.W. & La Spada, A.R. (2006) Thermoregulatory and metabolic defects in Huntington's disease transgenic mice implicate PGC-1alpha in Huntington's disease neurodegeneration. *Cell Metab.*, **4**, 349–362.
Wootz, H., Hansson, I., Korhonen, L. & Lindholm, D. (2006) XIAP decreases caspase-12 cleavage and calpain activity in spinal cord of ALS transgenic mice. *Exp. Cell Res.*, **312**, 1890–1898.
Ylikallio, E., Tyynismaa, H., Tsutsui, H., Ide, T. & Suomalainen, A. (2010) High mitochondrial DNA copy number has detrimental effects in mice. *Hum. Mol. Genet.*, **19**, 2695–2705.
Zheng, B., Liao, Z., Locascio, J.J., Lesniak, K.A., Roderick, S.S., Watt, M.L., Eklund, A.C., Zhang-James, Y., Kim, P.D., Hauser, M.A., Grünblatt, E., Moran, L.B., Mandel, S.A., Riederer, P., Miller, R.M., Federoff, H.J., Wüllner, U., Papapetropoulos, S., Youdim, M.B., Cantuti-Castelvetri, I., Young, A.B., Vance, J.M., Davis, R.L., Hedreen, J.C., Adler, C.H., Beach, T.G., Graeber, M.B., Middleton, F.A., Rochet, J.C., Scherzer, C.R. & Global PD Gene Expression (GPEX) Consortium (2010) PGC-1α, a potential therapeutic target for early intervention in Parkinson's disease. *Sci. Transl. Med.*, **2**, 52ra73.
Zhu, C., Xu, F., Fukuda, A., Wang, X., Fukuda, F., Korhonen, L., Hagberg, H., Lannering, B., Nilsson, M., Eriksson, P.S., Northington, F.J., Björk-Eriksson, T., Lindholm, D. & Blomgren, K. (2007) XIAP reduces oxidative stress after cerebral irradiation or hypoxia-ischemia through up-regulation of mitochondrial antioxidants. *Eur. J. Neurosci.*, **26**, 3402–3410.